

Multi-Compartment Variational Online Learning for Spiking Neural Networks

Hyeryung Jang and Osvaldo Simeone

Abstract

Spiking Neural Networks (SNNs) offer a novel computational paradigm that captures some of efficiency of biological brains for inference and learning via recursive processing and binary neural activations. Most existing training algorithms for SNNs assume spiking neuron models in which a neuron outputs individual spikes as a function of the dynamics of an internal state variable known as membrane potential. This paper explores a more general model in which each spiking neuron contains multiple compartments, each tracking the dynamics of a distinct membrane potential, while sharing the same synaptic weights across compartments. It is demonstrated that learning rules based on probabilistic generalized linear neural models can leverage the presence of multiple compartments through modern variational inference based on importance weighting or generalized expectation-maximization. The key idea is to use the neural compartments to sample multiple independent spiking signals from hidden neurons so as to obtain better statistical estimates of the likelihood training criterion. The derived online learning algorithms follow three-factor rules with global learning signals. Experimental results on a structured output memorization task and classification task with a standard neuromorphic data set demonstrate significant improvements in terms of accuracy and calibration with an increasing number of compartments.

I. INTRODUCTION

Background: Much of the recent progress towards solving pattern recognition tasks in complex domains, such as natural images, audio, and text, has relied on parametric models based on Artificial Neural Networks (ANNs). It has been widely reported that ANNs often yields learning

H. Jang and O. Simeone are with King's Communications, Learning, and Information Processing (KCLIP) lab at the Centre for Telecommunications Research in the Department of Engineering, King's College London, London, United Kingdom (emails: hyeryung.jang@kcl.ac.uk, osvaldo.simeone@kcl.ac.uk).

This work was supported by the European Research Council (ERC) under the European Union's Horizon 2020 Research and Innovation programme (Grant Agreement No. 725731).

and inference algorithms with prohibitive energy and time requirements [1], [2]. This has motivated a renewed interest in exploring novel computational paradigms that can capture the efficiency of biological brains for information encoding and processing.

The idea of neuromorphic computing – that is, of computing machines mimicking biological brains – dates back to the work by Carver Mead [3], and is currently being revisited both in terms of hardware and algorithm design. Neuromorphic computing platforms include IBM’s TrueNorth [4], Intel’s Loihi [5], and BrainChip’s Akida [6]. All these hardware solutions implement Spiking Neural Networks (SNNs) instead of ANNs. SNNs consist of biologically inspired neural units that process and communicate via sparse spiking signals over time, rather than via real numbers, over recurrent computing graphs [7]. Experimental evidence has confirmed the potential of SNNs implemented on neuromorphic chips in yielding energy consumption savings in many tasks of interest. For example, for a keyword spotting application, a Loihi-based implementation was reported to offer a $38.6\times$ improvement in energy cost per inference as compared to state-of-the-art ANNs (see Fig. 1 in [8]). Other related experimental findings concern the identification of odorant samples under contaminants [9] using SNNs via Loihi.

The design of training algorithms for SNNs needs to address the non-differentiable threshold crossing-triggered activation of spiking neurons [7] and the locality of the updates permitted by neuromorphic chips [5]. The non-differentiability problem can be tackled by smoothing out the activation function [10] or its derivative [7], or by relying on probabilistic models for spiking neurons [11]–[13]. In [7], [14], [15], credit assignment schemes such as random backpropagation, feedback alignment, or local randomized targets have been introduced in order to address locality for deterministic models. For probabilistic SNN models, credit assignment is directly derived in the form of a global learning signal through the optimization of a variational learning objective [11]–[13].

Motivation: All the algorithmic solutions reviewed above are based on a spiking neuron model in which neurons store and update an individual membrane potential. The membrane potential of a neuron evolves over time as a function of past spike signals from pre-synaptic neurons. In this paper, as illustrated in Fig. 1 and Fig. 2, we explore a more general model in which neurons have multiple compartments, with each compartment tracking a distinct membrane potential, all sharing the same synaptic weights. As we will demonstrate, this architecture can improve the performance of SNNs without increasing the number of model parameters. The approach

leverages probabilistic SNN models and variational inference methods.

In probabilistic neural networks, neurons spike with a probability that increases with the membrane potential. A simple way to leverage multiple compartments would be for ensembling at test time: for any given input, run independent realizations of the SNN’s spiking behavior in order to reduce the variance of its outputs, e.g., using a majority rule for classification. In this paper, we demonstrate that having multiple compartments during training can enhance the test performance even when a standard single-compartment SNN is deployed for testing.

To this end, the proposed approach tackles the challenge for the design of training algorithms in probabilistic models caused by the presence of “hidden” neurons (see Fig. 1). The key idea is that using multiple compartments can help reduce the variance caused by sampling for the hidden neurons, hence improving the estimate of the (likelihood) training criterion. To elaborate, we now provide some basic background.

Multi-sample training methods: In general, probabilistic machine learning models define a parameterized joint probability $p(\mathbf{x}, \mathbf{h})$ for observed variables \mathbf{x} and latent variables \mathbf{h} . Recent advances in variational inference (VI) have made it possible to train such models efficiently despite the presence of possibly high-dimensional hidden variables \mathbf{h} . VI refers to techniques that tackle the maximization of the marginal likelihood of the data, namely $\log p(\mathbf{x})$, through the maximization of the evidence lower bound (ELBO). The ELBO can be introduced via the following identity

$$\log p(\mathbf{x}) = \underbrace{\mathbb{E}_{q(\mathbf{h})} \left[\log \frac{p(\mathbf{x}, \mathbf{h})}{q(\mathbf{h})} \right]}_{\text{ELBO}} + \text{KL}(q(\mathbf{h}) || p(\mathbf{h}|\mathbf{x})), \quad (1)$$

where $q(\mathbf{h})$ is an arbitrary distribution, known as variational posterior, and the term $\text{KL}(p||q) = \sum_{\mathbf{x}} p(\mathbf{x}) \log \frac{p(\mathbf{x})}{q(\mathbf{x})} \geq 0$ represents the Kullback-Leibler divergence between distributions p and q . VI methods, mimicking the Expectation-Maximization (EM) algorithm [16], tackle the maximization of the ELBO by iteratively optimizing over the variational posterior $q(\mathbf{h})$ and over the model parameters defining the complete likelihood $p(\mathbf{x}, \mathbf{h})$. To this end, state-of-the-art VI methods evaluate expectations over the variational posterior $q(\mathbf{h})$ through MC sampling averages obtained by drawing samples $\mathbf{h} \sim q(\mathbf{h})$.

References [11]–[13], [17] derived learning rules for SNNs that optimize the ELBO for given observed spiking signals \mathbf{x} , with a variational posterior equal to the forward distribution of the

model. These techniques are based on a MC estimate of the ELBO that uses a single sample $\mathbf{h} \sim q(\mathbf{h})$ for the hidden neurons. This allows the learning rules to be implemented in online manner by simply running the network in feedforward mode over time.

In recent studies for ANNs, alternative approaches leveraging $K > 1$ samples from the variational posterior have been developed that optimize a more accurate lower bound on the marginal log-likelihood than the ELBO [18]–[21]. These lower bounds become tighter as the number K of samples increases, converging to the exact value $\log p(\mathbf{x})$ as $K \rightarrow \infty$. The resulting methods produce training algorithms based on importance weighting (IW) [18], [20], [21] or generalized EM (GEM) [19].

Main contributions: This paper sets out to investigate for the first time multi-sample learning rules for probabilistic SNNs. In order to enable the generation of multiple samples for the hidden neurons, we assume that spiking neurons in the SNN are endowed with K compartments, each implementing a separate Generalized Linear Model (GLM) [22] with shared weights across all compartments. We specifically develop VI online local learning rules for SNNs with multiple compartments that improve the learning and inference performance of state-of-the-art single-compartment Variational online Learning rules for SNNs (VLSNN) in [11]–[13]. As illustrated in Fig. 1, we focus on tasks that require to respond to exogeneous input spatio-temporal patterns by producing desired sequences of spiking signals at its output.

We introduce a number of new local, online, learning rules for multi-compartment SNNs. All rules are based on updates that use information local to each neuron, except for one or more learning signals computed from the collective behavior of a subset of the neurons following the general form of three-factor-rules [23].

- By leveraging the availability of K compartments during training, we first introduce a mini-batch variant of variational online learning for SNNs (MB-VLSNN) that uses a mini-batch of K samples for the hidden neurons to obtain a sample-averaging MC estimate of the gradient. This potentially reduces the variance of the gradient-based updates of the ELBO.
- We then design importance-weighted variational online learning (IW-VLSNN) rules that follow the principles of the importance weighting method in [18], [20], [21] to optimize an increasingly more accurate lower bound on the marginal log-likelihood as K increases. The learning rule IW-VLSNN applies different learning signals to hidden and visible neurons. A potential improvement is also introduced that applies per-compartment learning signals

(IW-VLSNN-b).

- We derive a new learning rule GEM-VLSNN based on GEM [19]. The rule applies the same per-compartment learning signals to all neurons based on approximate importance weights.
- We provide derivations and a study of the communication loads between neurons and the central controller for all rules.
- Finally, experimental results on standard neuromorphic data sets demonstrate the advantage of learning rules for probabilistic SNNs that leverage multiple compartments to improve training and test performance.

II. RELATED WORK

As discussed, most of the algorithmic solutions for SNNs have been studied by assuming that each spiking neuron emits individual spikes, i.e., single-compartment models [11]–[13], [17]. Several modelling and algorithmic approaches have been proposed to introduce and leverage multiple compartments per neuron. A line of work including [24]–[26] considers spiking Winner-Take-All (WTA) circuits. As the multi-compartment neurons investigated here, WTA circuits maintain multiple membrane potentials per circuit. Unlike the multi-compartment model, each potential is assigned to one of a group of spatially correlated spiking units in the circuit, and the potentials define a competitive process across the units through which at most one of the elements in the circuit spikes. To this end, in a WTA circuit, the weights used to compute each potential are different. This is essential in order to ensure that each element is sensitive to different spatio-temporal patterns. Therefore, increasing the number of WTA circuits entails a model with potentially more parameters, while increasing the number of compartments does not affect the model complexity.

Other related models assume more general interconnection among compartments in order to capture the dynamic behavior of branchy dendrites [27], [28]. In these models, dendritic structures are treated as multiple compartments coupled with each other. In [28], a network of spiking neurons, each with dendritic and somatic compartments, was studied to regulate both the average firing rates and the population sparseness via separate learning rules for the compartments. Compartmentalized structures can also be effectively simulated by neuromorphic hardware with support for multi-compartment dendrites on the SpiNNaker chip [29] and on Intel’s Loihi [5].

The idea of using such multi-sample objectives as a better proxy for the log-likelihood has been proposed for ANN-based variational autoencoders with continuous latent variables in [18].

This work used the reparameterization trick in order to reduce the variance of the estimator. In [19], the authors proposed an importance sampling based estimator or a generalized EM bound on the log-likelihood. Focusing on the model with discrete latent variables, an unbiased gradient estimator for a multi-sample objective with per-sample learning signals was derived in [20]. A theoretical connection between the multi-sample objective and the log-likelihood was discussed in [21].

III. MULTI-COMPARTMENT SNN MODEL

In a conventional probabilistic SNN, each neuron processes incoming spiking signals via given synaptic and somatic kernels and weights, producing a membrane potential that determines the spiking probability of the neuron [30]. In this section, we introduce the operational principles of a K -compartment SNN model that implements K parallel SNN models with shared synaptic and somatic weights. Accordingly, as illustrated in Fig. 2, all synapses and neurons have K compartments, with the output of the k th synaptic compartment being processed by the k th compartment of the post-synaptic neuron, for $k = 1, 2, \dots, K$. During *inference*, or testing, all compartments operate in parallel as conventional single-compartment SNNs, while *training* of the shared weights is carried out jointly across all compartments.

A. Inference

A K -compartment SNN model is defined here as a network connecting a set \mathcal{V} of spiking neurons, with each synapse and neuron having K compartments. As illustrated in Fig. 1, synapses are specified as the directed links of an arbitrary directed graph $\mathcal{G} = (\mathcal{V}, \mathcal{E})$, which may have cycles. Each k th synaptic compartment for a synapse $(i, j) \in \mathcal{E}$ processes the output of the k th compartment of the pre-synaptic neuron $i \in \mathcal{V}$; and its output is in turn processed by the k th compartment of the post-synaptic neuron j . During inference, the SNN operates as K parallel conventional probabilistic SNNs as follows.

Focusing on a discrete-time implementation, each spiking neuron i at discrete time $t = 1, 2, \dots$, outputs a binary value $s_{i,t}^k \in \{0, 1\}$, with “1” denoting the emission of a spike. The value $s_{i,t}^k$ is communicated to the post-synaptic neuron j through the k th compartment of synapse (i, j) , with $(i, j) \in \mathcal{E}$. We collect in vector $\mathbf{s}_t^k = (s_{i,t}^k : i \in \mathcal{V})$ the spikes of the k th compartment emitted by all neurons \mathcal{V} at time t , and denote by $\mathbf{s}_{\leq t}^k = (\mathbf{s}_1^k, \dots, \mathbf{s}_t^k)$ the spike sequences of all neurons

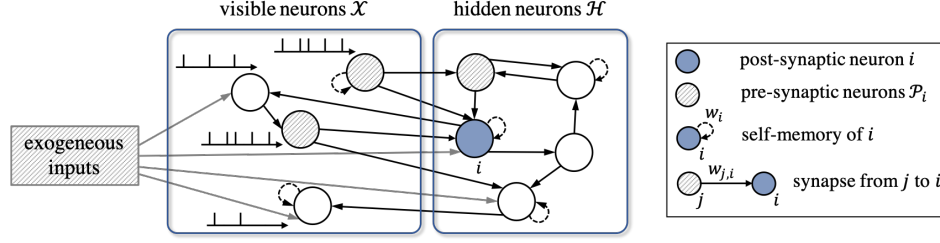


Fig. 1. Architecture of an SNN with exogenous inputs and $|\mathcal{X}| = 4$ visible and $|\mathcal{H}| = 5$ hidden spiking neurons – the directed links \mathcal{E} between two neurons represent synaptic dependencies, while the self-loop links represent self-memory. The directed graph \mathcal{G} may have loops, indicating recurrent behavior. Each neuron and synapse has K compartments (see Fig. 2).

in the compartment up to time t . Each post-synaptic neuron i receives past input spike signals $\mathbf{s}_{\mathcal{P}_i, \leq t-1}^k$ from the set \mathcal{P}_i of pre-synaptic neurons, which is defined by the parents of node i in graph \mathcal{G} , i.e., $\mathcal{P}_i = \{j \in \mathcal{V} : (j, i) \in \mathcal{E}\}$. With some abuse of notation, we include exogenous inputs to a neuron i (see Fig. 1) in the set \mathcal{P}_i of pre-synaptic neurons.

As illustrated in Fig. 2, for the k th compartment, independently of the other compartments, the spiking probability of neuron i at time t conditioned on its previous outputs and on the previous activity of its pre-synaptic neurons is defined as

$$p_{\theta_i}(s_{i,t}^k = 1 | \mathbf{s}_{\mathcal{P}_i, \leq t-1}^k, \mathbf{s}_{i, \leq t-1}^k) = p_{\theta_i}(s_{i,t}^k = 1 | u_{i,t}^k) = \sigma(u_{i,t}^k), \quad (2)$$

with $\sigma(x) = (1 + \exp(-x))^{-1}$ being the sigmoid function. The *membrane potential* $u_{i,t}^k$ summarizes the effect of past spike signals $\{\mathbf{s}_{\mathcal{P}_i, \leq t-1}^k, \mathbf{s}_{i, \leq t-1}^k\}$ from the pre-synaptic neurons \mathcal{P}_i and from the neuron i itself at the current time t . Note that each compartment stores and updates a distinct membrane potential. From (2), the spiking probability increases with the membrane potential, and the log-probability of the output $s_{i,t}^k \in \{0, 1\}$ corresponds to the binary negative cross-entropy, i.e.,

$$\log p_{\theta_i}(s_{i,t}^k | u_{i,t}^k) = \bar{H}(s_{i,t}^k, \sigma(u_{i,t}^k)) := s_{i,t}^k \log \sigma(u_{i,t}^k) + (1 - s_{i,t}^k) \log(1 - \sigma(u_{i,t}^k)). \quad (3)$$

The membrane potential $u_{i,t}^k$ is obtained as the output of spatio-temporal filters with inputs given by $\{\mathbf{s}_{\mathcal{P}_i, \leq t-1}^k, \mathbf{s}_{i, \leq t-1}^k\}$ [30], [31]. Specifically, given synaptic filter, or kernel, a_t and somatic filter, or kernel, b_t , each synapse $(j, i) \in \mathcal{E}$ from a pre-synaptic neuron $j \in \mathcal{P}_i$ to a post-synaptic

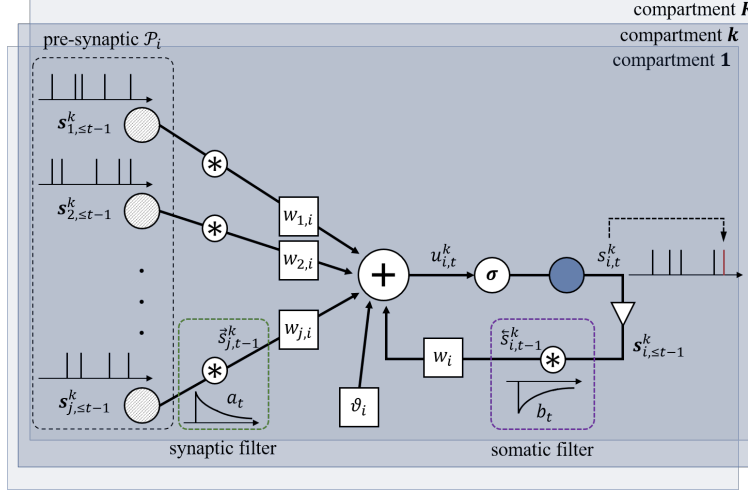


Fig. 2. Illustration of the membrane potential $u_{i,t}^k$ model for a multi-compartment SNN, with K compartments and exponential synaptic and somatic filters. At each compartment k within a neuron i , independently of all other compartments, the contribution of the k th synaptic trace from a pre-synaptic neuron $j \in \mathcal{P}_i$ through synaptic filter a_t are multiplied by the corresponding synaptic weights $w_{j,i}$, and the contribution of the k th somatic trace of a post-synaptic neuron i through self-memory filter b_t is multiplied by a weight w_i . The bias parameter ϑ_i is summed to obtain the membrane potential $u_{i,t}^k$, which is used to determine the spiking probability through the sigmoid function $\sigma(\cdot)$. Synaptic weights are shared among all compartments of a synapse, and similarly bias and feedback weight are shared among all compartments of a neuron.

neuron i computes the synaptic filtered trace

$$\overrightarrow{s}_{j,t}^k = a_t * s_{j,t}^k, \quad (4)$$

while the somatic filtered trace of neuron i is computed as $\overleftarrow{s}_{i,t}^k = b_t * s_{i,t}^k$, where we denote by $f_t * g_t$ the convolution operator $f_t * g_t = \sum_{\delta > 0} f_\delta g_{t-\delta}$. The synaptic and somatic kernels are common to all neurons and compartments. If the kernels are impulse responses of autoregressive filters, e.g., α -functions with parameters, then the filtered traces can be computed recursively without keeping track of windows of past spiking signals [32]. It is also possible to assign multiple kernels to each synapse [30].

The membrane potential of neuron i at time t is finally given as the weighted sum

$$u_{i,t}^k = \sum_{j \in \mathcal{P}_i} w_{j,i} \overrightarrow{s}_{j,t-1}^k + w_i \overleftarrow{s}_{i,t-1}^k + \vartheta_i, \quad (5)$$

where $w_{j,i}$ is a synaptic weight of the synapse (j, i) between pre-synaptic neuron $j \in \mathcal{P}_i$ and post-synaptic neuron i ; w_i is the “self-memory” weight; and ϑ_i is a bias parameter, with $\theta_i = \{\{w_{j,i}\}_{j \in \mathcal{P}_i}, w_i, \vartheta_i\}$ being the local model parameters of neuron i . As mentioned, parameter

vector θ_i is shared among all compartments of neuron i .

To summarize, during inference, given exogeneous inputs, all the compartments evolve independently over time t , with the k th compartment each neuron i spiking with probability (2). In more detail, as illustrated in Fig. 2, at each time t , given the incoming signals $\{s_{\mathcal{P}_i, \leq t-1}^k\}_{k=1}^K$ from all compartments of the pre-synaptic neurons \mathcal{P}_i (including the exogeneous inputs) and given the local model parameters θ_i of neuron i , each synapse (j, i) computes the K synaptic filtered traces $\{\vec{s}_{j, t-1}^k\}_{k=1}^K$. Neuron i computes the K somatic filtered traces $\{\overleftarrow{s}_{i, t-1}^k\}_{k=1}^K$. Then, for each compartment k within neuron i , the associated membrane potential $u_{i, t}^k$ is computed using the filtered traces $\{\{\vec{s}_{j, t-1}^k\}_{j \in \mathcal{P}_i}, \overleftarrow{s}_{i, t-1}^k\}$ as in (5), a spike $s_{i, t}^k$ is emitted with probability $\sigma(u_{i, t}^k)$.

Depending on the inference task, the spiking signals produced by the K compartments can be used in different ways to obtain the model's decision. For instance, in a classification task, as studied in Sec. VIII, a separate classification decision can be taken at each compartment and then a majority rule applied to output a final decision.

B. Training

As discussed, during inference, the SNN acts as a probabilistic sequence-to-sequence mapping between exogeneous inputs and outputs that is defined by the model parameters $\theta = \{\theta_i\}_{i \in \mathcal{V}}$. During training, the model parameters θ are adapted based on the available data with the goal of maximizing the likelihood of obtaining desired output sequences for given inputs. To elaborate, as illustrated in Fig. 1, we divide the neurons of SNN into the disjoint subsets of visible \mathcal{X} , and hidden, or latent, \mathcal{H} neurons, hence setting $\mathcal{V} = \mathcal{X} \cup \mathcal{H}$. The visible neurons encode the desired outputs, which are specified by the training data as spiking vector sequences $\mathbf{x}_{\leq T}^k$ for some $T > 0$. These can be generally different across distinct compartment $k = 1, \dots, K$. In contrast, the spiking signals of the hidden neurons, denoted as $\mathbf{h}_{\leq T}^k$ for each compartment k , are unspecified, and should be adapted to ensure the desired behavior of the visible neurons. Using the notation in Sec. III-A, during learning, we set $s_{i, t}^k = x_{i, t}^k$ for each compartment of a visible neuron $i \in \mathcal{X}$. We also use the notation $s_{i, t}^k = h_{i, t}^k$ for each compartment of any hidden neuron $i \in \mathcal{H}$, as well as $\mathbf{s}_t^k = (\mathbf{x}_t^k, \mathbf{h}_t^k)$ for the overall set of spike signals processed by the compartment k of all neurons at time t .

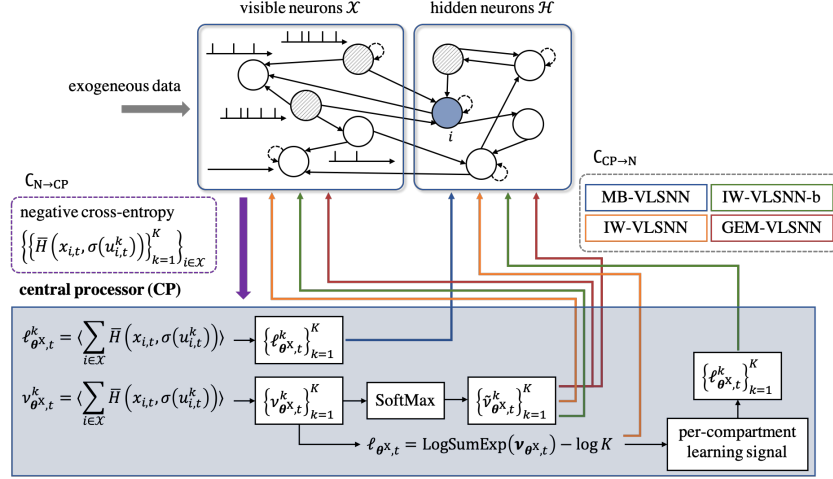


Fig. 3. Illustration of the architecture and communication paths for the considered training schemes for a multi-compartment SNN. Learnable model parameters θ are adapted based on data fed into the visible neurons \mathcal{X} with the help of the stochastic spiking behavior of hidden neurons \mathcal{H} . For all learning rules, a central processor (CP) collects (periodically or at each time step) information from all compartments of the visible neurons, with entailing a communication load $C_{N \rightarrow CP}$ (quantified in Table. I); it computes learning signals; and it sends them to either only to the hidden neurons or to both hidden and visible neurons, with entailing a communication load $C_{CP \rightarrow N}$, in order to guide the update of model parameters.

As a common learning criterion in probabilistic models [33], we focus on maximizing the log-likelihood that visible neurons in set \mathcal{X} output the desired spiking behavior $\mathbf{x}_{\leq T}^k$ in response to given exogeneous inputs. Mathematically, the problem is written as the maximum likelihood (ML) problem

$$\max_{\theta} \sum_{k=1}^K \log p_{\theta}(\mathbf{x}_{\leq T}^k), \quad (6)$$

where the log-likelihood of the data $\mathbf{x}_{\leq T}^k$ is obtained via marginalization over the hidden spiking signals $\mathbf{h}_{\leq T}^k$ as $\log p_{\theta}(\mathbf{x}_{\leq T}^k) = \log \sum_{\mathbf{h}_{\leq T}^k} p_{\theta}(\mathbf{x}_{\leq T}^k, \mathbf{h}_{\leq T}^k)$. This marginalization would require summing over the $2^{|\mathcal{H}|T}$ possible values of the hidden neurons, which is practically infeasible.

This paper is concerned with the derivation of online local learning rules that tackle the ML problem (6). The general form of the desired online training rule for multi-compartment SNNs follows the standard three-factor format implemented by most neuromorphic hardware [5], [23]: A synaptic weight $w_{j,i}$ from pre-synaptic neuron j to a post-synaptic neuron i is updated as

$$w_{j,i} \leftarrow w_{j,i} + \eta \cdot \sum_{k=1}^K \ell^k \cdot \langle \text{pre}_j^k \cdot \text{post}_i^k \rangle, \quad (7)$$

where η is the learning rate and $\langle \cdot \rangle$ denotes a time-averaging operator. The update (7) sums the contributions from the K compartments, with each contribution depending on three different factors. The term pre_j^k is a function of the filtered traces (4) for the (j, i) synapse, hence depending only on the spiking signals of the pre-synaptic neuron j , while the factor post_i^k depends on the activity of the post-synaptic neuron i processed by the k th compartment. Finally, ℓ^k is a scalar *learning signal* that determines the sign and magnitude of the contribution of the k th compartment to the learning update. The learning signal can generally be evaluated by a central processor that has access to the current outputs $(\mathbf{x}_t^k, \mathbf{h}_t^k)$ of the SNN. The learning signal ℓ^k may be missing in some learning rules for given subset of neurons (see Fig. 3 for a preview).

IV. SINGLE-COMPARTMENT VARIATIONAL ONLINE LEARNING FOR SNNs

In this section, we review the online learning algorithm introduced in [11]–[13] that tackles the ML problem in (6) for $K = 1$ by using stochastic gradient descent (SGD). Since we focus on the special case of a single compartment, i.e., $K = 1$, we drop the dependence on the superscript k in this section. Throughout the paper, we define the temporal average operator of a time sequence $\{f_t\}_{t \geq 1}$ with some constant $\kappa \in (0, 1)$ as $\langle f_t \rangle_\kappa = \kappa \cdot \langle f_{t-1} \rangle_\kappa + f_t$ with $\langle f_0 \rangle_\kappa = 0$.

A. VLSNN: Variational Online Learning for SNNs

In online learning, the model parameters $\boldsymbol{\theta}$ are updated at each time t based on the data $\mathbf{x}_{\leq t}$ observed so far. To this end, at each time $t = 1, 2, \dots$, the visible neurons are clamped to the data \mathbf{x}_t , and each hidden neuron $i \in \mathcal{H}$ emits a spike $h_{i,t} = 1$ with probability $\sigma(u_{i,t})$ from (2). Weights updates are carried out using a three-factor rule of the form (7) as follows. A central processor (CP) collects the binary negative cross-entropy values $\bar{H}(x_{i,t}, \sigma(u_{i,t}))$ in (3) from all visible neurons $i \in \mathcal{X}$, and it computes the learning signal

$$\ell_{\boldsymbol{\theta}^x, t} = \left\langle \sum_{i \in \mathcal{X}} \bar{H}(x_{i,t}, \sigma(u_{i,t})) \right\rangle_\gamma, \quad (8)$$

for some constant $\gamma \in (0, 1)$. The learning signal is then fed back from the CP to all hidden neurons \mathcal{H} . Finally, each neuron i updates the local model parameters θ_i as

$$\vartheta_i \leftarrow \vartheta_i + \eta \cdot \begin{cases} \langle x_{i,t} - \sigma(u_{i,t}) \rangle_\gamma, & \text{if } i \in \mathcal{X} \\ (\ell_{\theta^x,t} - b_t^{\vartheta_i}) \cdot \langle h_{i,t} - \sigma(u_{i,t}) \rangle_\kappa, & \text{if } i \in \mathcal{H} \end{cases} \quad (9a)$$

$$w_{j,i} \leftarrow w_{j,i} + \eta \cdot \begin{cases} \langle (x_{i,t} - \sigma(u_{i,t})) \cdot \vec{s}_{j,t-1} \rangle_\gamma, & \text{if } i \in \mathcal{X} \\ (\ell_{\theta^x,t} - b_t^{w_{j,i}}) \cdot \langle (h_{i,t} - \sigma(u_{i,t})) \cdot \vec{s}_{j,t-1} \rangle_\kappa, & \text{if } i \in \mathcal{H} \end{cases} \quad (9b)$$

$$w_i \leftarrow w_i + \eta \cdot \begin{cases} \langle (x_{i,t} - \sigma(u_{i,t})) \cdot \overleftarrow{x}_{i,t-1} \rangle_\gamma, & \text{if } i \in \mathcal{X} \\ (\ell_{\theta^x,t} - b_t^{w_i}) \cdot \langle (h_{i,t} - \sigma(u_{i,t})) \cdot \overleftarrow{h}_{i,t-1} \rangle_\kappa, & \text{if } i \in \mathcal{H} \end{cases} \quad (9c)$$

with a constant $\kappa \in (0, 1)$. The baselines $\mathbf{b}_{i,t} = \{\{b_t^{w_{j,i}}\}_{j \in \mathcal{P}_i}, b_t^{w_i}, b_t^{\vartheta_i}\}$ are control variates introduced as means to minimize the variance of the gradient estimator for hidden neuron $i \in \mathcal{H}$. Following the approach in [34], the optimized baseline can be evaluated as

$$\mathbf{b}_{i,t} = \frac{\langle \ell_{\theta^x,t} \cdot \mathbf{e}_{i,t}^2 \rangle_{\kappa_b}}{\langle \mathbf{e}_{i,t}^2 \rangle_{\kappa_b}},$$

for some constant $\kappa_b \in (0, 1)$, with $\mathbf{e}_{i,t} = \langle \nabla_{\theta_i} \bar{H}(h_{i,t}, \sigma(u_{i,t})) \rangle_\kappa$ denoting the *eligibility trace* of neuron i at time t . We refer to the online rule (9) as Variational online Learning for SNNs (VLSNN).

B. Derivation of VLSNN

In order to make the paper self-contained and to facilitate the derivation of multi-compartment learning schemes, we present here a brief derivation of VLSNN. To address the ML problem (6) in an online manner, VLSNN aims at maximizing at each time t a discounted version of a lower bound $L_{\mathbf{x}_{\leq T}}(\boldsymbol{\theta})$ on the log-likelihood $\log p_{\boldsymbol{\theta}}(\mathbf{x}_{\leq T})$ of the observation $\mathbf{x}_{\leq T}$. Using Jensen's inequality, the lower bound is obtained as

$$\begin{aligned} \log p_{\boldsymbol{\theta}}(\mathbf{x}_{\leq T}) &= \log \sum_{\mathbf{h}_{\leq T}} p_{\boldsymbol{\theta}}(\mathbf{x}_{\leq T}, \mathbf{h}_{\leq T}) \\ &\geq \mathbb{E}_{\mathbf{h}_{\leq T} \sim p_{\boldsymbol{\theta}^H}(\mathbf{h}_{\leq T} | \mathbf{x}_{\leq T-1})} \left[\sum_{t=1}^T \sum_{i \in \mathcal{X}} \bar{H}(x_{i,t}, \sigma(u_{i,t})) \right] := L_{\mathbf{x}_{\leq T}}(\boldsymbol{\theta}), \end{aligned} \quad (10)$$

where we have used the notation

$$p_{\theta^H}(\mathbf{h}_{\leq T} | \mathbf{x}_{\leq T-1}) = \prod_{t=1}^T p_{\theta}(\mathbf{h}_t | \mathbf{x}_{\leq t-1}, \mathbf{h}_{\leq t-1}) = \prod_{t=1}^T \prod_{i \in \mathcal{H}} p_{\theta_i}(h_{i,t} | u_{i,t}) \quad (11)$$

to indicate the causally conditioned distribution of hidden neurons, signals given the visible neurons, signals [35]. We note that we have the decomposition

$$p_{\theta}(\mathbf{x}_{\leq T}, \mathbf{h}_{\leq T}) = p_{\theta^H}(\mathbf{h}_{\leq T} | \mathbf{x}_{\leq T-1}) p_{\theta^X}(\mathbf{x}_{\leq T} | \mathbf{h}_{\leq T-1}),$$

where the causally conditioned distribution of visible neuron given hidden neurons is similarly defined as $p_{\theta^X}(\mathbf{x}_{\leq T} | \mathbf{h}_{\leq T-1}) = \prod_{t=1}^T \prod_{i \in \mathcal{X}} p_{\theta_i}(x_{i,t} | u_{i,t})$ [35]. We denote as $\theta^X = \{\theta_i\}_{i \in \mathcal{X}}$ and $\theta^H = \{\theta_i\}_{i \in \mathcal{H}}$ the collection of model parameters for visible \mathcal{X} and hidden \mathcal{H} neurons, respectively. Finally, we define the time-discounted version of the lower bound $L_{\mathbf{x}_{\leq T}}(\theta)$ in (10) at time t as

$$L_{\mathbf{x}_{\leq t}}(\theta) = \mathbb{E}_{\mathbf{h}_{\leq t} \sim p_{\theta^H}(\mathbf{h}_{\leq t} | \mathbf{x}_{\leq t-1})} \left[\underbrace{\sum_{t'=0}^{t-1} \gamma^{t'} \sum_{i \in \mathcal{X}} \bar{H}(x_{i,t-t'}, \sigma(u_{i,t-t'}))}_{:= \ell_{\theta^X, t}} \right], \quad (12)$$

where $0 < \gamma < 1$ is a discount factor.

The online local update rule VLSNN in (9) can be obtained by maximizing the lower bound $L_{\mathbf{x}_{\leq t}}(\theta)$ in (12) via SGD in the direction of a stochastic estimate of the gradient $\nabla_{\theta} L_{\mathbf{x}_{\leq t}}(\theta)$. The gradient of (12) is obtained from the standard REINFORCE gradient, which is estimated by drawing a single spiking signal $\mathbf{h}_{\leq t} \sim p_{\theta^H}(\mathbf{h}_{\leq t} | \mathbf{x}_{\leq t-1})$ for the hidden neurons from the causally conditioned distribution (11). Note that, as explained in Sec. I, the limitation of a single sample is dictated by the presence of single-compartment neurons, i.e., $K = 1$. The resulting MC estimate of the gradient can be computed as [13]

$$\nabla_{\theta} L_{\mathbf{x}_{\leq t}}(\theta) = \sum_{t'=0}^{t-1} \gamma^{t'} \sum_{i \in \mathcal{X}} \nabla_{\theta} \bar{H}(x_{i,t-t'}, \sigma(u_{i,t-t'})) + \ell_{\theta^X, t} \cdot \sum_{t'=1}^t \sum_{i \in \mathcal{H}} \nabla_{\theta} \bar{H}(h_{i,t'}, \sigma(u_{i,t'})), \quad (13)$$

which yields the SGD-based learning rule as $\theta \leftarrow \theta + \eta \cdot \nabla_{\theta} L_{\mathbf{x}_{\leq t}}(\theta)$ with a learning rate η . This can be seen to coincide with (9) [11]–[13].

C. Interpreting VLSNN

Following the discussion around (7), the update rule (9) has the form of a three-factor rule [23] and is local, with the exception of the learning signal $\ell_{\theta^X, t}$ used for the update of hidden

neurons' parameters. For each neuron i , the gradients $\nabla_{\theta_i} L_{\mathbf{x}_{\leq t}}(\boldsymbol{\theta})$ with respect to the local model parameters $\boldsymbol{\theta}_i$ from (13) contain three types of terms, namely the post-synaptic error $s_{i,t} - \sigma(u_{i,t})$ and post-synaptic feedback trace $\overleftarrow{s}_{i,t-1}$; pre-synaptic synaptic trace $\overrightarrow{s}_{j,t-1}$; and the common global learning signal $\ell_{\boldsymbol{\theta}^x,t}$ in (8). For hidden neurons \mathcal{H} , the learning signal is used to guide the update, while the visible neurons \mathcal{X} do not use the learning signal. The common learning signal term $\ell_{\boldsymbol{\theta}^x,t}$ in (8) can then be interpreted as indicating how effective the current, randomly sampled, behavior of hidden neurons $\mathbf{h}_{\leq t}$ is in ensuring the maximization of the likelihood of the desired observation $\mathbf{x}_{\leq t}$ for the visible neurons.

D. Communication Load

As discussed, VLSNN requires bi-directional communication. As seen in Fig. 3, at each step t , first, unicast communication from visible neurons to CP is required in order to compute the learning signal $\ell_{\boldsymbol{\theta}^x,t}$ by collecting information $\{\bar{H}(x_{i,t}, \sigma(u_{i,t}))\}_{i \in \mathcal{X}}$ from all visible neurons. The resulting unicast communication load, from neurons to CP, is $C_{\mathcal{N} \rightarrow \text{CP}}^{(K=1)} = |\mathcal{X}|$ real numbers. The learning signal is then sent back to all hidden neurons, resulting a broadcast communication load from CP to neurons equal to $C_{\text{CP} \rightarrow \mathcal{N}}^{(K=1)} = |\mathcal{H}|$ real numbers.

V. MINI-BATCH VARIATIONAL ONLINE LEARNING FOR SNNs

As discussed, VLSNN is based on a MC estimate of the gradient $\nabla_{\boldsymbol{\theta}} L_{\mathbf{x}_{\leq t}}(\boldsymbol{\theta})$ of the likelihood function that relies on a single stochastic sample $\mathbf{h}_{\leq t}$ for the hidden neurons. This constraint is dictated by the availability of a single compartment. The gradient used by VLSNN has a generally high variance, only partially decreased by the presence of the baseline control variates in (9). In this section, we introduce a first learning rule that leverages multiple compartments to potentially improve the learning performance of VLSNN by reducing the variance of the gradient-based updates.

A. MB-VLSNN: Mini-batch Variational Online Learning for SNNs

As anticipated in Sec. I, in order to reduce the variance of the MC estimate in (9), it is possible to use a mini-batch of K samples from the causally conditioned distribution (11) by leveraging the availability of K compartments. The resulting mini-batch variational online learning for SNNs (MB-VLSNN) operates as follows.

In a K -compartment SNN, at each time $t = 1, 2, \dots$, each compartment k within the visible neurons are clamped to the respective entry in data $\mathbf{x}_{\leq t}^k$. Each hidden neuron $i \in \mathcal{H}$ outputs K binary values $\{h_{i,t}^k\}_{k=1}^K$, with the k th compartment emitting a spike $h_{i,t}^k = 1$ with probability $\sigma(u_{i,t}^k)$ in (2). The model parameters are updated in online manner as follows. The CP collects the binary negative cross-entropy values $\{\bar{H}(x_{i,t}^k, \sigma(u_{i,t}^k))\}_{k=1}^K$ of all compartments from all visible neurons $i \in \mathcal{X}$ in order to compute the *per-compartment* learning signal $\ell_{\theta^x,t}^k$ as in (8), with $u_{i,t} = u_{i,t}^k$, for the k th compartment. The learning signals $\{\ell_{\theta^x,t}^k\}_{k=1}^K$ are then fed back from the CP to all hidden neurons \mathcal{H} . The communication paths are illustrated in Fig. 3.

Finally, for each neuron i , MB-VLSNN updates the local model parameters θ_i by averaging the VLSNN updates in (9) over the generated K samples as

$$\vartheta_i \leftarrow \vartheta_i + \eta \cdot \begin{cases} \frac{1}{K} \cdot \sum_{k=1}^K \langle x_{i,t}^k - \sigma(u_{i,t}^k) \rangle_{\gamma}, & \text{if } i \in \mathcal{X} \\ \frac{1}{K} \cdot \sum_{k=1}^K (\ell_{\theta^x,t}^k - b_t^{\vartheta_i,k}) \cdot \langle h_{i,t}^k - \sigma(u_{i,t}^k) \rangle_{\kappa}, & \text{if } i \in \mathcal{H} \end{cases} \quad (14a)$$

$$w_{j,i} \leftarrow w_{j,i} + \eta \cdot \begin{cases} \frac{1}{K} \cdot \sum_{k=1}^K \langle (x_{i,t}^k - \sigma(u_{i,t}^k)) \cdot \vec{s}_{j,t-1}^k \rangle_{\gamma}, & \text{if } i \in \mathcal{X} \\ \frac{1}{K} \cdot \sum_{k=1}^K (\ell_{\theta^x,t}^k - b_t^{w_{j,i},k}) \cdot \langle (h_{i,t}^k - \sigma(u_{i,t}^k)) \cdot \vec{s}_{j,t-1}^k \rangle_{\kappa}, & \text{if } i \in \mathcal{H} \end{cases} \quad (14b)$$

$$w_i \leftarrow w_i + \eta \cdot \begin{cases} \frac{1}{K} \cdot \sum_{k=1}^K \langle (x_{i,t}^k - \sigma(u_{i,t}^k)) \cdot \overleftarrow{x}_{i,t-1} \rangle_{\gamma}, & \text{if } i \in \mathcal{X} \\ \frac{1}{K} \cdot \sum_{k=1}^K (\ell_{\theta^x,t}^k - b_t^{w_i,k}) \cdot \langle (h_{i,t}^k - \sigma(u_{i,t}^k)) \cdot \overleftarrow{h}_{i,t-1}^k \rangle_{\kappa}, & \text{if } i \in \mathcal{H} \end{cases} \quad (14c)$$

with time-averaging constants $\gamma, \kappa \in (0, 1)$. We note that, in the update rule (14), the relevance of each sample $\mathbf{h}_{\leq t}^k$ of the hidden neurons depends on the k th learning signal $\ell_{\theta^x,t}^k$. In similar manner to VLSNN, for each hidden neuron $i \in \mathcal{H}$, per-compartment baseline $\mathbf{b}_{i,t}^k$ can be optimized to minimize the variance (due to the magnitude of the per-compartment learning signal) as [34]

$$\mathbf{b}_{i,t}^k = \frac{\langle \ell_{\theta^x,t}^k \cdot (\mathbf{e}_{i,t}^k)^2 \rangle_{\kappa_b}}{\langle (\mathbf{e}_{i,t}^k)^2 \rangle_{\kappa_b}},$$

for some constant $\kappa_b \in (0, 1)$, with $\mathbf{e}_{i,t}^k = \langle \nabla_{\theta_i} \bar{H}(h_{i,t}^k, \sigma(u_{i,t}^k)) \rangle_{\kappa}$ being the eligibility trace at the k th compartment of neuron i at time t .

B. Communication Load

As seen in Fig. 3, MB-VLSNN requires computation of K learning signals at CP, the resulting communication loads increase linearly to K . Specifically, the unicast communication load from

neurons to CP is $C_{N \rightarrow CP} = K C_{N \rightarrow CP}^{(K=1)} = K|\mathcal{X}|$ real numbers; while the broadcast communication load from CP to neurons is $C_{CP \rightarrow N} = K C_{CP \rightarrow N}^{(K=1)} = K|\mathcal{H}|$ real numbers.

VI. IMPORTANCE-WEIGHTED VARIATIONAL ONLINE LEARNING FOR SNNs

The MB-VLSNN rule introduced above leverages the K compartments to improve the MC estimate of the gradient $\nabla_{\theta} L_{\mathbf{x}_{\leq T}}(\theta)$ of the lower bound (10) of the log-likelihood $\log p_{\theta}(\mathbf{x}_{\leq T})$. In this section, we consider an alternative approach that uses multiple compartments to obtain an increasingly more accurate bound on the log-likelihood. The approach follows the principles of the importance weighting method introduced in [18], [20], [21] for conventional probabilistic models.

A. Importance-Weighted Evidence Lower Bound

In order to introduce a tighter bound on the log-likelihood, we start by considering the importance-weighted estimator of the likelihood $p_{\theta}(\mathbf{x}_{\leq T}) = \mathbb{E}_{\mathbf{h}_{\leq T} \sim p_{\theta H}(\mathbf{h}_{\leq T} || \mathbf{x}_{\leq T-1})} \left[\frac{p_{\theta}(\mathbf{x}_{\leq T}, \mathbf{h}_{\leq T})}{p_{\theta H}(\mathbf{h}_{\leq T} || \mathbf{x}_{\leq T-1})} \right]$ given as

$$R_K = \frac{1}{K} \sum_{k=1}^K \frac{p_{\theta}(\mathbf{x}_{\leq T}, \mathbf{h}_{\leq T}^k)}{p_{\theta H}(\mathbf{h}_{\leq T}^k || \mathbf{x}_{\leq T-1})}, \quad \text{with } \mathbf{h}_{\leq T}^{1:K} \sim p_{\theta H}(\mathbf{h}_{\leq T}^{1:K} || \mathbf{x}_{\leq T-1}). \quad (15)$$

The estimator (15) uses K independent samples $\mathbf{h}_{\leq T}^{1:K} = \{\mathbf{h}_{\leq T}^k\}_{k=1}^K$ from the hidden neurons drawn from the causally conditioned distribution (11), where we accordingly introduced the joint distribution $p_{\theta H}(\mathbf{h}_{\leq T}^{1:K} || \mathbf{x}_{\leq T-1}) = \prod_{k=1}^K p_{\theta H}(\mathbf{h}_{\leq T}^k || \mathbf{x}_{\leq T-1})$. The estimator (15) is unbiased, i.e., $p_{\theta}(\mathbf{x}_{\leq T}) = \mathbb{E}_{p_{\theta H}(\mathbf{h}_{\leq T}^{1:K} || \mathbf{x}_{\leq T-1})} [R_K]$. Using this estimator along with Jensen's inequality, we can then obtain the multi-sample lower bound on the log-likelihood

$$\log p_{\theta}(\mathbf{x}_{\leq T}) = \log \mathbb{E}[R_K] \geq \mathbb{E}[\log R_K] := L_{\mathbf{x}_{\leq T}}^K(\theta), \quad (16)$$

where the expectation is over the distribution $p_{\theta H}(\mathbf{h}_{\leq T}^{1:K} || \mathbf{x}_{\leq T-1})$. Plugging (15) into (16), the lower bound (16) can be rewritten as

$$\begin{aligned} \log p_{\theta}(\mathbf{x}_{\leq T}) &= \log \mathbb{E}_{p_{\theta H}(\mathbf{h}_{\leq T}^{1:K} || \mathbf{x}_{\leq T-1})} \left[\frac{1}{K} \sum_{k=1}^K \exp(w_{\theta^x}^k) \right] \\ &\geq \mathbb{E}_{p_{\theta H}(\mathbf{h}_{\leq T}^{1:K} || \mathbf{x}_{\leq T-1})} \left[\log \frac{1}{K} \sum_{k=1}^K \exp \left(\sum_{t=1}^T w_{\theta^x, t}^k \right) \right] = L_{\mathbf{x}_{\leq T}}^K(\theta), \end{aligned} \quad (17)$$

where we have defined the log-weight of each sample k as

$$w_{\theta^x}^k = \log p_{\theta^x}(\mathbf{x}_{\leq T} | \mathbf{h}_{\leq T-1}^k) = \sum_{t=1}^T \sum_{i \in \mathcal{X}} \log p_{\theta_i}(x_{i,t} | u_{i,t}^k) = \sum_{t=1}^T \underbrace{\sum_{i \in \mathcal{X}} \bar{H}(x_{i,t}, \sigma(u_{i,t}^k))}_{:= w_{\theta^x,t}^k}. \quad (18)$$

If $K > 1$, the importance-weighted lower bound $L_{\mathbf{x}_{\leq T}}^K(\boldsymbol{\theta})$ in (17) is guaranteed to be tighter than the standard ELBO $L_{\mathbf{x}_{\leq T}}(\boldsymbol{\theta})$, which is a special case with $K = 1$. Furthermore, for $K \rightarrow \infty$, the lower bound $L_{\mathbf{x}_{\leq T}}^K(\boldsymbol{\theta})$ converges to the exact log-likelihood $\log p_{\theta}(\mathbf{x}_{\leq T})$ [18].

In order to obtain an online learning rule, we aim at maximizing at each time t a discounted version of the lower bound $L_{\mathbf{x}_{\leq T}}^K(\boldsymbol{\theta})$ defined as

$$L_{\mathbf{x}_{\leq t}}^K(\boldsymbol{\theta}) = \mathbb{E}_{\mathbf{h}_{\leq t}^{1:K} \sim p_{\theta^H}(\mathbf{h}_{\leq t}^{1:K} | \mathbf{x}_{\leq t-1})} \left[\underbrace{\log \frac{1}{K} \sum_{k=1}^K \exp \left(\underbrace{\sum_{t'=0}^{t-1} \gamma^{t'} w_{\theta^x,t-t'}^k}_{:= v_{\theta^x,t}^k} \right)}_{:= \ell_{\theta^x,t}} \right], \quad (19)$$

where $0 < \gamma < 1$ is a discount factor.

B. IW-VLSNN: Importance-Weighted Variational Online Learning for SNNs

In this section, we develop an online local learning rule that maximizes the importance-weighted lower bound $L_{\mathbf{x}_{\leq t}}^K(\boldsymbol{\theta})$ in (19). We refer to the rule as Importance-Weighted Variational online Learning for SNNs (IW-VLSNN). IW-VLSNN updates the model parameters $\boldsymbol{\theta}$ via SGD in the direction of the gradient $\nabla_{\boldsymbol{\theta}} L_{\mathbf{x}_{\leq t}}^K(\boldsymbol{\theta})$, which is obtained using REINFORCE as

$$\begin{aligned} \nabla_{\boldsymbol{\theta}} L_{\mathbf{x}_{\leq t}}^K(\boldsymbol{\theta}) = \mathbb{E}_{p_{\theta^H}(\mathbf{h}_{\leq t}^{1:K} | \mathbf{x}_{\leq t-1})} & \left[\sum_{k=1}^K \tilde{v}_{\theta^x,t}^k \cdot \sum_{t'=0}^{t-1} \gamma^{t'} \sum_{i \in \mathcal{X}} \nabla_{\boldsymbol{\theta}} \bar{H}(x_{i,t-t'}, \sigma(u_{i,t-t'}^k)) \right. \\ & \left. + \ell_{\theta^x,t} \cdot \sum_{k=1}^K \sum_{t'=1}^t \sum_{i \in \mathcal{H}} \nabla_{\boldsymbol{\theta}} \bar{H}(h_{i,t'}^k, \sigma(u_{i,t'}^k)) \right]. \end{aligned} \quad (20)$$

In (20), we have defined $\mathbf{v}_{\theta^x,t} = (v_{\theta^x,t}^1, \dots, v_{\theta^x,t}^K)$ as the vector of unnormalized log-weights of the samples at time t in (19) using temporal average operator as

$$v_{\theta^x,t}^k = \langle w_{\theta^x,t}^k \rangle_{\gamma} = \left\langle \sum_{i \in \mathcal{X}} \bar{H}(x_{i,t}, \sigma(u_{i,t}^k)) \right\rangle_{\gamma}, \quad (21a)$$

and the normalized weights $\tilde{\mathbf{v}}_{\theta^{\mathbf{x}},t} = (\tilde{v}_{\theta^{\mathbf{x}},t}^1, \dots, \tilde{v}_{\theta^{\mathbf{x}},t}^K)$ are defined using the SoftMax function over K samples as

$$\tilde{\mathbf{v}}_{\theta^{\mathbf{x}},t} = \text{SoftMax}(\mathbf{v}_{\theta^{\mathbf{x}},t}), \quad \text{where} \quad \tilde{v}_{\theta^{\mathbf{x}},t}^k = \text{SoftMax}^k(\mathbf{v}_{\theta^{\mathbf{x}},t}) = \frac{\exp(v_{\theta^{\mathbf{x}},t}^k)}{\sum_{k'=1}^K \exp(v_{\theta^{\mathbf{x}},t}^{k'})}. \quad (21b)$$

The learning signal $\ell_{\theta^{\mathbf{x}},t}$ at time t in (19) can be expressed using the LogSumExp function as

$$\ell_{\theta^{\mathbf{x}},t} = \text{LogSumExp}(\mathbf{v}_{\theta^{\mathbf{x}},t}) - \log K, \quad \text{where} \quad \text{LogSumExp}(\mathbf{v}_{\theta^{\mathbf{x}},t}) = \log \sum_{k=1}^K \exp(v_{\theta^{\mathbf{x}},t}^k). \quad (21c)$$

The resulting learning algorithm IW-VLSNN based on the MC estimate of the gradient (20) operates as follows.

In a K -compartment SNN, at each time $t = 1, 2, \dots$, all compartments within visible neurons are clamped to the data $\mathbf{x}_{\leq t}$, while each hidden neuron $i \in \mathcal{H}$ emits a spike $h_{i,t}^k = 1$ with probability $\sigma(u_{i,t}^k)$ at each compartment $k = 1, \dots, K$. Then, the model parameters are updated as follows. As illustrated in Fig. 3, the CP collects the binary negative cross-entropy values $\{\bar{H}(x_{i,t}, \sigma(u_{i,t}^k))\}_{k=1}^K$ of all compartments from all visible neurons $i \in \mathcal{X}$. These are used by the CP to compute the importance weights $\mathbf{v}_{\theta^{\mathbf{x}},t}$ from (21a); the normalized importance weights $\tilde{\mathbf{v}}_{\theta^{\mathbf{x}},t}$ in (21b); and the learning signal $\ell_{\theta^{\mathbf{x}},t}$ from (21c). Finally, the normalized weights $\{\tilde{v}_{\theta^{\mathbf{x}},t}^k\}_{k=1}^K$ are fed back from the CP to all visible neurons \mathcal{X} , while a common learning signal $\ell_{\theta^{\mathbf{x}},t}$ is fed back to all hidden neurons \mathcal{H} . Finally, for each neuron i , IW-VLSNN updates the local model parameters θ_i as

$$\vartheta_i \leftarrow \vartheta_i + \eta \cdot \begin{cases} \sum_{k=1}^K \tilde{v}_{\theta^{\mathbf{x}},t}^k \cdot \langle x_{i,t} - \sigma(u_{i,t}^k) \rangle_{\gamma}, & \text{if } i \in \mathcal{X} \\ (\ell_{\theta^{\mathbf{x}},t} - b_t^{\vartheta_i}) \cdot \sum_{k=1}^K \langle h_{i,t}^k - \sigma(u_{i,t}^k) \rangle_{\kappa}, & \text{if } i \in \mathcal{H} \end{cases} \quad (22a)$$

$$w_{j,i} \leftarrow w_{j,i} + \eta \cdot \begin{cases} \sum_{k=1}^K \tilde{v}_{\theta^{\mathbf{x}},t}^k \cdot \langle (x_{i,t} - \sigma(u_{i,t}^k)) \cdot \vec{s}_{j,t-1}^k \rangle_{\gamma}, & \text{if } i \in \mathcal{X} \\ (\ell_{\theta^{\mathbf{x}},t} - b_t^{w_{j,i}}) \cdot \sum_{k=1}^K \langle (h_{i,t}^k - \sigma(u_{i,t}^k)) \cdot \vec{s}_{j,t-1}^k \rangle_{\kappa}, & \text{if } i \in \mathcal{H} \end{cases} \quad (22b)$$

$$w_i \leftarrow w_i + \eta \cdot \begin{cases} \sum_{k=1}^K \tilde{v}_{\theta^{\mathbf{x}},t}^k \cdot \langle (x_{i,t} - \sigma(u_{i,t}^k)) \cdot \overleftarrow{x}_{i,t-1} \rangle_{\gamma}, & \text{if } i \in \mathcal{X} \\ (\ell_{\theta^{\mathbf{x}},t} - b_t^{w_i}) \cdot \sum_{k=1}^K \langle (h_{i,t}^k - \sigma(u_{i,t}^k)) \cdot \overleftarrow{h}_{i,t-1}^k \rangle_{\kappa}, & \text{if } i \in \mathcal{H} \end{cases} \quad (22c)$$

with constants $\gamma, \kappa \in (0, 1)$. For each hidden neuron $i \in \mathcal{H}$, the baseline $\mathbf{b}_{i,t}$ can be introduced

to minimize the variance of the gradient estimator (20) as [34]

$$\mathbf{b}_{i,t} = \frac{\langle \ell_{\theta^x,t} \cdot \sum_{k=1}^K (e_{i,t}^k)^2 \rangle_{\kappa_b}}{\langle \sum_{k=1}^K (e_{i,t}^k)^2 \rangle_{\kappa_b}}. \quad (23)$$

for some constant $\kappa_b \in (0, 1)$.

C. Interpreting IW-VLSNN

The update rule (22) follows the three-factor format in (7). The dependence on the post-synaptic error, post-synaptic feedback trace, and pre-synaptic synaptic trace is applied for each compartment as for VLSNN and MB-VLSNN, while the learning signal is given in different form to each neuron. For visible neurons, the normalized importance weights $\{\tilde{v}_{\theta^x,t}^k\}_{k=1}^K$ are given as learning signals, with the contribution of each compartment being weighted by $\tilde{v}_{\theta^x,t}^k$. From (21b), the normalized weight $\tilde{v}_{\theta^x,t}^k$ measures the relative effectiveness of the random realizations of the hidden neurons within the k th compartment in reproducing the desired behavior of the visible neurons. In contrast, for the hidden neurons, the learning signal $\ell_{\theta^x,t}$ in (21c) is given as a global feedback, indicating how effective their current overall behavior across all compartments is in ensuring the maximization of the likelihood of observation $\mathbf{x}_{\leq t}$. Note that this signal is shared across all compartments.

D. Communication Load

From the description of IW-VLSNN given above, as illustrated in Fig. 3, the unicast communication load of IW-VLSNN from neuron to CP is $C_{N \rightarrow CP} = K C_{N \rightarrow CP}^{(K=1)} = K|\mathcal{X}|$ real numbers; while the broadcast communication load from CP to neurons is $C_{CP \rightarrow N} = K|\mathcal{X}| + |\mathcal{H}|$. As compared to MB-VLSNN whose broadcast load is $K|\mathcal{H}|$, the broadcast communication load of IW-VLSNN can be smaller if the number of hidden neurons is large.

E. IW-VLSNN with Per-Compartment Learning Signal

As per (22), IW-VLSNN applies the same baseline (23) to all compartments of the hidden neurons. Hence, unlike the differentiated per-compartment feedback signals sent to the visible neurons, IW-VLSNN does not implement relative credit assignment across the K compartments for hidden neurons. The common learning signal applied to each compartment may not be sufficiently specific and, as a result, it may suffer from high variance. In order to address this

TABLE I
LEARNING COMMUNICATION LOADS (IN REAL NUMBERS)

SCHEME	UNICAST COMM LOAD $C_{N \rightarrow CP}$	BROADCAST COMM LOAD $C_{CP \rightarrow N}$
VLSNN	$C_{N \rightarrow CP}^{(K=1)} = \mathcal{X} $	$C_{CP \rightarrow N}^{(K=1)} = \mathcal{H} $
MB-VLSNN	$K \mathcal{X} $	$K \mathcal{H} $
IW-VLSNN	$K \mathcal{X} $	$K \mathcal{X} + \mathcal{H} $
IW-VLSNN-B	$K \mathcal{X} $	$K(\mathcal{X} + \mathcal{H})$
GEM-VLSNN	$K \mathcal{X} $	$K(\mathcal{X} + \mathcal{H})$

issue, we introduce per-compartment learning signals denoted by $\ell_{\theta^x,t}^k$ for all compartments $k = 1, \dots, K$ of the hidden neurons. Following [20], a per-compartment learning signal can be defined by subtracting a term dependent on the contribution of the other compartments to the learning signal in (19) as

$$\ell_{\theta^x,t}^k = \ell_{\theta^x,t} - \log \frac{1}{K} \left(\sum_{k' \neq k} \exp(v_{\theta^x,t}^{k'}) + \exp\left(\frac{1}{K-1} \sum_{k' \neq k} v_{\theta^x,t}^{k'}\right) \right).$$

With this approach, the CP needs to compute the per-compartment learning signals $\{\ell_{\theta^x,t}^k\}_{k=1}^K$ with information collected from the visible neurons \mathcal{X} , which are then fed back to all hidden neurons \mathcal{H} . Instead of the update rule (22), this alternative rule, referred to as IW-VLSNN-b, updates the local model parameters θ_i of each neuron i as

$$\theta_i \leftarrow \theta_i + \eta \cdot \begin{cases} \sum_{k=1}^K \tilde{v}_{\theta^x,t}^k \cdot \langle \nabla_{\theta_i} \bar{H}(x_{i,t}, \sigma(u_{i,t}^k)) \rangle_{\gamma}, & \text{if } i \in \mathcal{X} \\ \sum_{k=1}^K \ell_{\theta^x,t}^k \cdot \langle \nabla_{\theta_i} \bar{H}(h_{i,t}, \sigma(u_{i,t}^k)) \rangle_{\kappa}, & \text{if } i \in \mathcal{H}. \end{cases} \quad (24)$$

As a result, as illustrated in Fig. 3, the broadcast communication load from CP to neurons includes the normalized weights of the compartments $\{\tilde{v}_{\theta^x,t}^k\}_{k=1}^K$ to visible neurons and $\{\ell_{\theta^x,t}^k\}_{k=1}^K$ per-compartment learning signals to hidden neurons, entailing the load $C_{CP \rightarrow N} = K(|\mathcal{X}| + |\mathcal{H}|)$.

VII. GENERALIZED EM VARIATIONAL ONLINE LEARNING FOR SNNs

In this section, we propose an alternative approach to leverage the available K compartments by following the generalized EM (GEM) method introduced in [19]. The learning algorithms discussed in previous sections can be interpreted as applications of a variational EM strategy that bypasses the M-step by substituting the causally conditioned distribution (11) for the learnable posterior of the hidden neurons (see [13] for details). In contrast, the approach considered here

tackles the M-step through an approximation of the posterior distribution of the hidden neurons that uses the samples generated by the K compartments to carry out marginalization. The resulting online learning rule, which we refer to Generalized EM Variational online Learning for SNNs (GEM-VLSNN), operates as described in the next section.

A. GEM-VLSNN: Generalized EM Variational Online Learning for SNNs

As illustrated in Fig. 3, at each time $t = 1, 2, \dots$, the CP collects the binary negative cross-entropy values $\{\bar{H}(x_{i,t}, \sigma(u_{i,t}^k))\}_{k=1}^K$ of all compartments from all visible neurons $i \in \mathcal{X}$ in order to compute the importance weights of the compartments $v_{\theta^x,t}$ as in (21a) with a constant $\kappa \in (0, 1)$, and computes the normalized weights $\tilde{v}_{\theta^x,t}$ using the SoftMax function as in (21b). Then, the normalized weights $\{\tilde{v}_{\theta^x,t}^k\}_{k=1}^K$ are fed back from the CP to all neurons \mathcal{V} (both visible \mathcal{X} and hidden \mathcal{H}). Finally, for each neuron i , GEM-VLSNN updates the local model parameters θ_i as

$$\vartheta_i \leftarrow \vartheta_i + \eta \cdot \sum_{k=1}^K \tilde{v}_{\theta^x,t}^k \cdot \langle s_{i,t}^k - \sigma(u_{i,t}^k) \rangle_\gamma, \quad (25a)$$

$$w_{j,i} \leftarrow w_{j,i} + \eta \cdot \sum_{k=1}^K \tilde{v}_{\theta^x,t}^k \cdot \langle (s_{i,t}^k - \sigma(u_{i,t}^k)) \cdot \vec{s}_{j,t-1}^k \rangle_\gamma, \quad (25b)$$

$$w_i \leftarrow w_i + \eta \cdot \sum_{k=1}^K \tilde{v}_{\theta^x,t}^k \cdot \langle (s_{i,t}^k - \sigma(u_{i,t}^k)) \cdot \overleftarrow{s}_{i,t-1}^k \rangle_\gamma, \quad (25c)$$

with constants $\gamma, \kappa \in (0, 1)$. In (25), we set $s_{i,t}^k = x_{i,t}$ for visible neuron $i \in \mathcal{X}$ and $s_{i,t}^k = h_{i,t}^k$ for hidden neuron $i \in \mathcal{H}$. We note that, unlike the schemes considered above, the same update rule is applied for both visible and hidden neurons.

B. Derivation of GEM-VLSNN

In the M-step of the EM algorithm, given the current iterate θ_{old} , one aims at maximizing the expected log-likelihood $\mathbb{E}_{p_{\theta_{\text{old}}}(\mathbf{h}_{\leq T} | \mathbf{x}_{\leq T})} [\log p_{\theta}(\mathbf{x}_{\leq T}, \mathbf{h}_{\leq T})] := L_{\mathbf{x}_{\leq T}}(\theta, \theta_{\text{old}})$, where the expectation is taken with respect to the posterior distribution $p_{\theta_{\text{old}}}(\mathbf{h}_{\leq T} | \mathbf{x}_{\leq T})$ in the E-step (see, e.g., [36], [37]). GEM approximates the output of the M-step by updating the model parameters θ via SGD in the direction of an estimate of the gradient $\nabla_{\theta} L_{\mathbf{x}_{\leq T}}(\theta, \theta_{\text{old}})$. Building on the GEM

approach, in order to obtain an online learning rule, we aim at maximizing at each time t the discounted version of the lower bound $L_{\mathbf{x}_{\leq T}}(\boldsymbol{\theta}, \boldsymbol{\theta}_{\text{old}})$ given as

$$L_{\mathbf{x}_{\leq t}}(\boldsymbol{\theta}, \boldsymbol{\theta}_{\text{old}}) = \mathbb{E}_{p_{\boldsymbol{\theta}_{\text{old}}}(\mathbf{h}_{\leq t}|\mathbf{x}_{\leq t})} \left[\sum_{t'=0}^{t-1} \gamma^{t'} \sum_{i \in \mathcal{V}} \bar{H}(s_{i,t-t'}, \sigma(u_{i,t-t'})) \right]. \quad (26)$$

We then approximate the learning criterion (26) as

$$\begin{aligned} L_{\mathbf{x}_{\leq t}}(\boldsymbol{\theta}, \boldsymbol{\theta}_{\text{old}}) &\approx \mathbb{E}_{p_{\boldsymbol{\theta}_{\text{old}}}(\mathbf{h}_{\leq t}^{1:K}|\mathbf{x}_{\leq t-1})} \left[\sum_{k=1}^K \text{SoftMax}^k \left(\sum_{t'=1}^t \mathbf{w}_{\boldsymbol{\theta}_{\text{old}}, t'}^{\mathbf{x}} \right) \cdot \sum_{t'=0}^{t-1} \gamma^{t'} \sum_{i \in \mathcal{V}} \bar{H}(s_{i,t-t'}^k, \sigma(u_{i,t-t'}^k)) \right] \\ &:= L_{\mathbf{x}_{\leq t}}^K(\boldsymbol{\theta}, \boldsymbol{\theta}_{\text{old}}), \end{aligned} \quad (27)$$

where $0 < \gamma < 1$ is a discount factor. In order to obtain the discounted lower bound $L_{\mathbf{x}_{\leq t}}^K(\boldsymbol{\theta}, \boldsymbol{\theta}_{\text{old}})$ in (27), in a manner similar to [19], an approximation of the expectation over the posterior is obtained by using K independent samples $\mathbf{h}_{\leq t}^{1:K} \sim p_{\boldsymbol{\theta}_{\text{old}}}(\mathbf{h}_{\leq t}^{1:K}|\mathbf{x}_{\leq t-1})$ from the causally conditioned distribution and computing the approximate importance weight

$$\frac{p_{\boldsymbol{\theta}}(\mathbf{h}_{\leq t}^k|\mathbf{x}_{\leq t})}{p_{\boldsymbol{\theta}^{\text{H}}}(\mathbf{h}_{\leq t}^k|\mathbf{x}_{\leq t-1})} = \frac{p_{\boldsymbol{\theta}}(\mathbf{x}_{\leq t}, \mathbf{h}_{\leq t}^k)}{p_{\boldsymbol{\theta}}(\mathbf{x}_{\leq t}) \cdot p_{\boldsymbol{\theta}^{\text{H}}}(\mathbf{h}_{\leq t}^k|\mathbf{x}_{\leq t-1})} \approx \frac{p_{\boldsymbol{\theta}^{\text{X}}}(\mathbf{x}_{\leq t}|\mathbf{h}_{\leq t-1}^k)}{\frac{1}{K} \sum_{k'=1}^K p_{\boldsymbol{\theta}^{\text{X}}}(\mathbf{x}_{\leq t}|\mathbf{h}_{\leq t-1}^{k'})}. \quad (28)$$

Hence, the set of K samples $\mathbf{h}_{\leq t}^{1:K}$ is used in (28) for an MC approximation of the marginal likelihood $p_{\boldsymbol{\theta}}(\mathbf{x}_{\leq t})$. With notation $w_{\boldsymbol{\theta}^{\text{X}}, t}^k$ in (18), we obtain the lower bound $L_{\mathbf{x}_{\leq t}}^K(\boldsymbol{\theta}, \boldsymbol{\theta}_{\text{old}})$ in (27).

An online local update rule GEM-VLSNN is obtained by maximizing the bound $L_{\mathbf{x}_{\leq t}}^K(\boldsymbol{\theta}, \boldsymbol{\theta}_{\text{old}})$ in (27) via SGD in the direction of the gradient $\nabla_{\boldsymbol{\theta}} L_{\mathbf{x}_{\leq t}}^K(\boldsymbol{\theta}, \boldsymbol{\theta}_{\text{old}})$. The gradient $\nabla_{\boldsymbol{\theta}} L_{\mathbf{x}_{\leq t}}^K(\boldsymbol{\theta}, \boldsymbol{\theta}_{\text{old}})$ with respect to the model parameters $\boldsymbol{\theta}$ is given by

$$\nabla_{\boldsymbol{\theta}} L_{\mathbf{x}_{\leq t}}^K(\boldsymbol{\theta}, \boldsymbol{\theta}_{\text{old}}) = \mathbb{E}_{p_{\boldsymbol{\theta}^{\text{H}}}(\mathbf{h}_{\leq t}^{1:K}|\mathbf{x}_{\leq t-1})} \left[\sum_{k=1}^K \tilde{v}_{\boldsymbol{\theta}^{\text{X}}, t}^k \cdot \sum_{t'=0}^{t-1} \gamma^{t'} \sum_{i \in \mathcal{V}} \nabla_{\boldsymbol{\theta}} \bar{H}(s_{i,t-t'}^k, \sigma(u_{i,t-t'}^k)) \right],$$

where the log-weights of the compartments $\mathbf{v}_{\boldsymbol{\theta}^{\text{X}}, t}$ at time t are defined by using temporal average operator (as in (21a)) with a constant $\kappa \in (0, 1)$ and the normalized weights $\tilde{v}_{\boldsymbol{\theta}^{\text{X}}, t}$ in (21b). This yields the SGD-based learning rule (25) as $\boldsymbol{\theta} \leftarrow \boldsymbol{\theta} + \eta \cdot \nabla_{\boldsymbol{\theta}} L_{\mathbf{x}_{\leq t}}^K(\boldsymbol{\theta})$ with a learning rate η .

C. Communication Load

In GEM-VLSNN, the unicast communication load from neurons to CP is $C_{\text{N} \rightarrow \text{CP}} = K C_{\text{N} \rightarrow \text{CP}}^{(K=1)} = K|\mathcal{X}|$ real numbers; while the broadcast communication load from CP to neurons is $C_{\text{CP} \rightarrow \text{N}} =$

$K(|\mathcal{X}| + |\mathcal{H}|)$. As compared to schemes considered in previous sections, the broadcast communication load of GEM-VLSNN and IW-VLSNN-b is the largest. We refer to Table I for a comparison of all learning schemes.

VIII. EXPERIMENTS

In this section, we evaluate the performance of the introduced schemes MB-VLSNN, IW-VLSNN, IW-VLSNN-b, and GEM-VLSNN on memorization and classification tasks defined on the neuromorphic data set MNIST-DVS [38]. We conduct experiments by varying the number K of compartments, which may be different during training and inference. We evaluate performance in terms of log-likelihood, classification accuracy, number of spikes [4], communication load, and calibration [39].

The *MNIST-DVS data set* was generated by displaying slowly-moving handwritten digit images from the MNIST data set on an LCD monitor and by recording the output of a DVS camera [40]. For each pixel of an image, positive or negative events are recorded when the pixel's luminosity respectively increases or decreases by more than a given amount, and no event is recorded otherwise. In this experiment, images are cropped to 26×26 pixels, and uniform downsampling over time is carried out to obtain $T = 80$ time samples per each image as in [41], [42]. The training data set is composed of 900 examples per each digit, from 0 to 9, and the test data set is composed of 100 examples per digit. The signs of the spiking signals are discarded, producing a binary, i.e., spiking, signal per pixel as in e.g., [41].

Throughout this section, as illustrated in Fig. 2, we consider a generic, non-optimized, network architecture characterized by a set of $|\mathcal{H}|$ fully connected hidden neurons, all receiving the exogeneous inputs as pre-synaptic signals, and a read-out visible layer, directly receiving pre-synaptic signals from all exogeneous inputs and all hidden neurons without recurrent connections between visible neurons. For synaptic and somatic filters, following the approach [30], we choose a set of three raised cosine functions with a synaptic duration of 10 time steps as synaptic filters, and, for somatic filter, we choose a single raised cosine function with duration of 10 time steps.

A. Memorization Task

We first focus on a structured output memorization task, which involves predicting the 13×26 spiking signals encoding the lower half of an MNIST-DVS digit from the 13×26 spiking

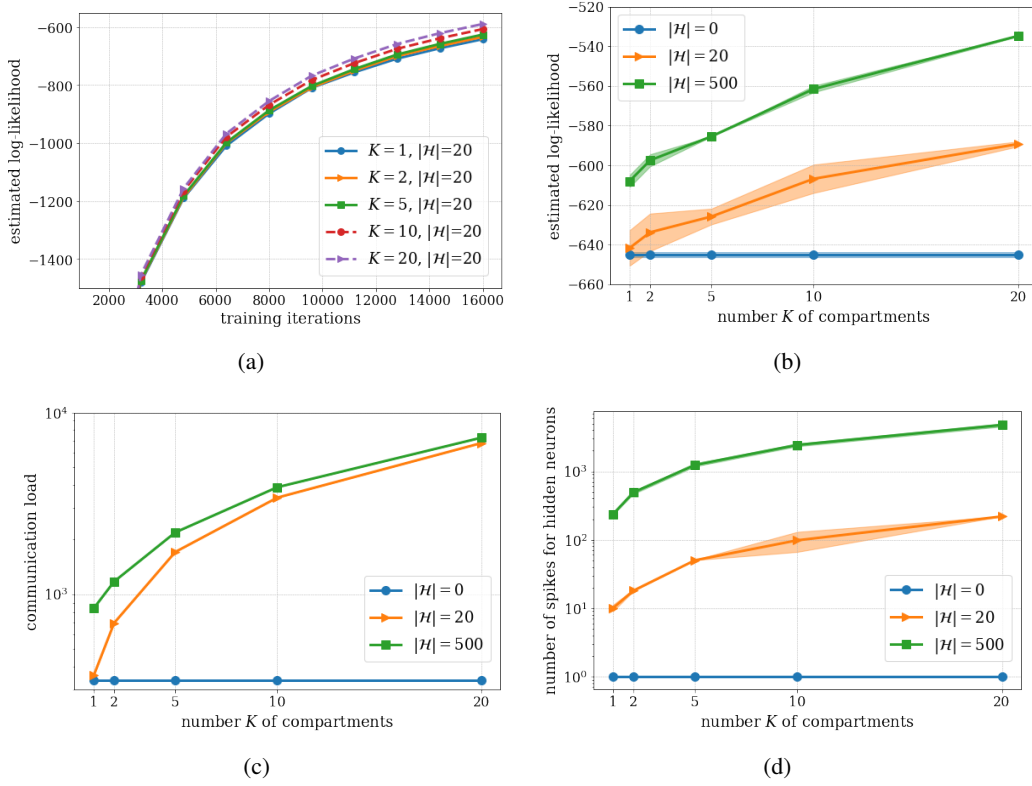


Fig. 4. Structured output memorization task trained on a single MNIST-DVS data point using IW-VLSNN: (a) (Estimated) log-likelihood of the desired output as a function of the number of processed time samples for different values of the number $K = 1, 2, 5, 10, 20$ of compartments with $|\mathcal{H}| = 20$. (b) (Estimated) log-likelihood for the desired output; (c) broadcast communication load $C_{CP \rightarrow N}$ from CP to neurons in Table I; and (d) number of spikes emitted by the hidden neurons per unit time during training as a function of the number K of compartments in training for different values of $|\mathcal{H}| = 20, 500$. Also shown for reference is the performance with $|\mathcal{H}| = 0$ and shaded areas represent 95% confidence intervals.

signals encoding its top half. The top-half spiking signals are given as exogeneous inputs to the SNN, while the lower-half spiking signals are assigned as the desired outputs $\mathbf{x}_{\leq T}$ for all the compartments of the $13 \times 26 = 338$ visible neurons, i.e., we set $\mathbf{x}_{\leq T}^k = \mathbf{x}_{\leq T}$ for all $k = 1, \dots, K$.

For this memorization task, we consider the case in which the multiple compartments are used *only for training*, while a single-compartment SNN with the trained weights is used for testing. In this case, the accuracy of an SNN model with parameter vector θ on a desired output signal $\mathbf{x}_{\leq T}$ is measured by the marginal log-likelihood $\log p_{\theta}(\mathbf{x}_{\leq T})$ obtained from (6) with $K = 1$. This quantity represents the log-probability that the conventional single-compartment SNN model assigns to sequence $\mathbf{x}_{\leq T}$. The log-likelihood is estimated via the empirical average of the negative cross entropy of the visible neurons over 20 independent realizations of the hidden neurons.

At a first example, we train a K -compartment SNN model by using IW-VLSNN during 200

consecutive presentations of a single MNIST-DVS training data point $\mathbf{x}_{\leq T}$, yielding a sequence of $200 \times T = 16000$ time samples. Similar results were obtained with the other proposed schemes. The trained SNN is tested on the same image, hence evaluating the capability of the SNN for memorization [12]. For training, hyperparameters such as learning rate η and time constants κ, γ have been selected after a non-exhaustive manual search and are shared among all learning schemes and experiments. The initial learning rate $\eta = 0.0005$ is decayed as $\eta = \eta / (1 + 0.2)$ every 40 presentations of the data point, and we set $\kappa = \gamma = 0.9$.

To start, Fig. 4(a) shows the evolution of the estimated log-likelihood of the desired output (the lower-half image) as more samples are processed by the proposed IW-VLSNN rule for different values of the number $K = 1, 2, 5, 10, 20$ of compartments and for $|\mathcal{H}| = 0, 20, 500$ hidden neurons. The corresponding estimated log-likelihood at the end of training is illustrated as a function of K in Fig. 4(c). It can be observed that using more compartments K improves the training performance due to the optimization of increasingly tighter bound on the likelihood. Improvements are also observed with an increasing number $|\mathcal{H}|$ of hidden neurons. However, it should be emphasized that increasing the number of hidden neurons increases proportionally the number of weights in the SNN, while a larger K does not increase the complexity of the model in terms of number of weights.

We now turn our attention to the requirements of the SNN trained with IW-VLSNN in terms of the communication load and of the number of spikes for hidden neurons during training. Fig. 4(d) shows the broadcast communication load $C_{CP \rightarrow N}$ from CP to neurons (see Table I for details) as a function of K for different values of $|\mathcal{H}|$. The communication load of an SNN trained using IW-VLSNN increases linearly with K and $|\mathcal{H}|$. Furthermore, a larger K implies a proportionally larger number of spikes emitted by the hidden neurons during training, as seen in Fig. 4(b). From Fig. 4, the proposed IW-VLSNN is seen to enable a flexible trade-off between communication load and energy consumption, on the one hand, and training performance, on the other, by leveraging the availability of K compartments.

B. Classification Task

Next, we consider a handwritten digit classification task based on the MNIST-DVS data set. We consider a multi-compartment SNN with 3 visible neurons in the read-out layer, one for each class of three digits ‘0’, ‘1’, and ‘2’. The 26×26 spiking signals encoding an MNIST-DVS

digit are given as exogeneous inputs to the SNN, while the digit labels $\{0, 1, 2\}$ are encoded by the neurons in the read-out layer. We train a K -compartment SNN model with $|\mathcal{H}| = 200$ on the 2700 training data points of digits $\{0, 1, 2\}$ by using all proposed schemes, and the SNN is tested on the 300 test data points. For training, we set the constant learning rate $\eta = 0.001$ and time constants $\kappa = \gamma = 0.9$, which have been selected after a non-exhaustive manual search and are shared among all learning schemes. We set $\mathbf{x}_{\leq T}^k = \mathbf{x}_{\leq T}$ for all $k = 1, \dots, K$, and the output neuron $c \in \mathcal{X}$ corresponding to the correct label is assigned a desired output spike signals $x_{c,t} = 1$, while the other neurons $c' \neq c$ are assigned $x_{c',t} = 0$ for $t = 1, \dots, T$.

For testing, a K^I -compartment SNN with the trained weights is used for inference. To this end, we adopt a standard majority decoding rule: for each compartment $k = 1, \dots, K^I$, the output neuron with the largest number of output spikes for each $\mathbf{x}_{\leq T}^k$ is selected, obtaining the decision $\hat{c}^k := \arg \max_{c \in \mathcal{X}} \sum_{t=1}^T x_{c,t}^k$; then the index of the output neuron that receives the most votes is set to the predicted class as

$$\hat{c} = \arg \max_{c \in \mathcal{X}} z_c, \quad (29a)$$

where $z_c = \sum_{k=1}^{K^I} \mathbb{1}_{\{\hat{c}^k=c\}}$ is the number of votes for class c .

In addition to accuracy, we will also consider *calibration* as a performance metric. To this end, the prediction probability \hat{p} , or confidence, of a decision is derived from the vote count variables $\mathbf{z} = (z_c : c \in \mathcal{X})$ using the SoftMax function, i.e.,

$$\hat{p} = \text{SoftMax}^{\hat{c}}(\mathbf{z}). \quad (29b)$$

The expected calibration error (ECE) measures the difference in expectation between confidence and accuracy, i.e.,

$$\text{ECE} = \mathbb{E}_{\hat{p}} \left[\left| \mathbb{P}(\hat{c} = c | \hat{p} = p) - p \right| \right]. \quad (30)$$

In (30), the probability $\mathbb{P}(\hat{c} = c | \hat{p} = p)$ is the probability that \hat{c} is the correct decision for inputs that yield accuracy $\hat{p} = p$. The ECE can be estimated by using quantization and empirical averages as detailed in [39].

To start, we plot in Fig. 5 the test accuracy, ECE, and estimated log-likelihood of the desired output spikes as a function of the number of training iterations. A larger K is seen to improve the test log-likelihood thanks to the optimization of a tighter bound on the training log-likelihood.

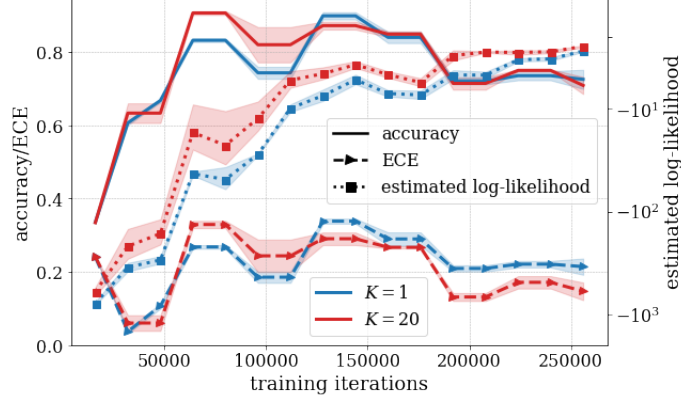


Fig. 5. Classification task trained on MNIST-DVS data points of digits $\{0, 1, 2\}$: Estimated log-likelihood, classification accuracy and expected calibration error (ECE) (30) of test data points as a function of processed time samples for different values K of compartments in training using GEM-VLSNN. The accuracy and ECE are measured using $K^I = 2$ compartments. The shaded areas represent 95% confidence intervals.

The larger log-likelihood also translates into a model that more accurately reproduces conditional probability of outputs given inputs [39], [43], which in turn enhances calibration. In contrast, accuracy can be improved with a larger K but only if regularization via early stopping is carried out. This points to the fact that the goal of maximizing the likelihood of specific desired output spiking signals is not equivalent to minimizing the classification error.

Finally, we provide a comparison among the proposed training schemes. We trained a K -compartment SNN and tested the SNN with $K^I = K$ compartments using all schemes, and the corresponding estimated log-likelihood, accuracy, broadcast communication load and the number of spikes for hidden neurons during training are illustrated as a function of K in Fig. 6. We recall that the proposed training schemes use learning signals for visible and hidden neurons in different ways. For visible neurons, MB-VLSNN does not differentiate among the contributions of different compartments, while other methods weigh them according to different normalized importance weights. For hidden neurons, IW-VLSNN uses *per-parameter* learning signal which is shared across all compartments; while IW-VLSNN-b and GEM-VLSNN use *per-compartment* learning signals; and MB-VLSNN applies *per-compartment* and *per-parameter* learning signal.

From Fig. 6, we first observe that GEM-VLSNN outperforms other methods for $K > 1$ in terms of test log-likelihood, accuracy, and number of spikes, while requiring the largest broadcast communication load $C_{CP \rightarrow N}$. Focusing on the impact of learning signals used for visible neurons, it is seen that using the normalized importance weights in IW-VLSNN, IW-VLSNN-b

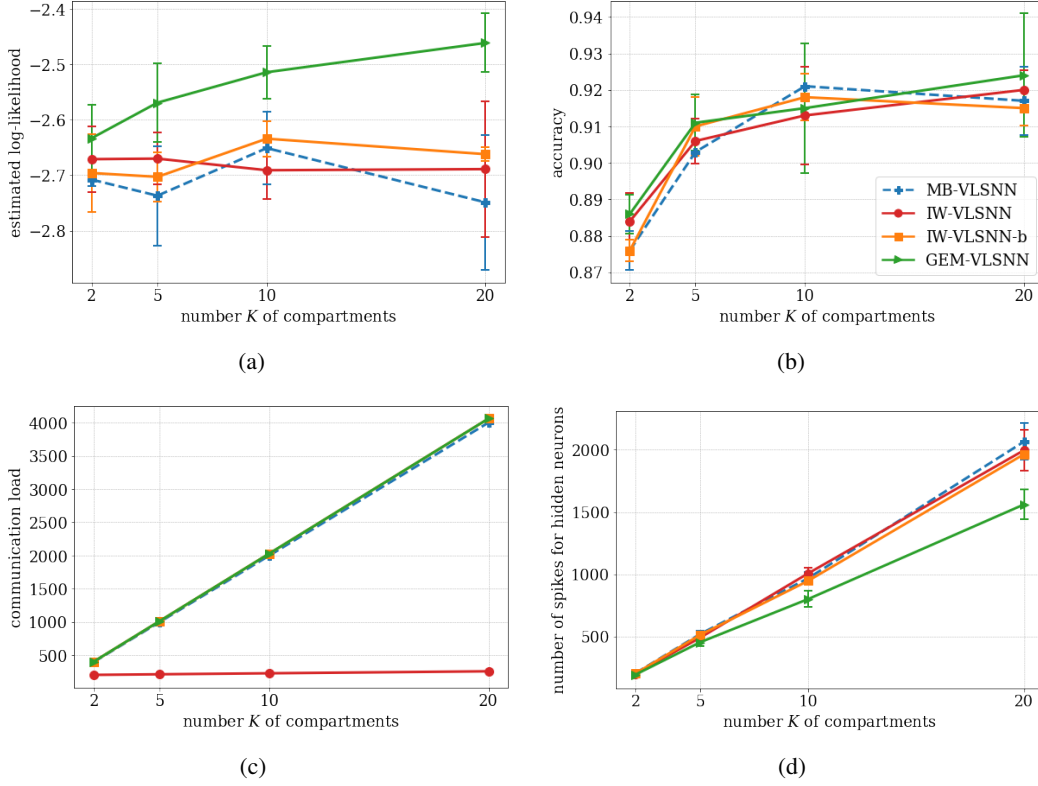


Fig. 6. Classification task trained on MNIST-DVS data set using MB-VLSNN, IW-VLSNN, IW-VLSNN-b and GEM-VLSNN versus K , with 95% confidence intervals accounting for the error bars: (a) (estimated) log-likelihood for the desired output on test data set; (b) classification accuracy of the test data set; (c) broadcast communication load $C_{CP \rightarrow N}$ from CP to neurons in Table I; and (d) number of spikes emitted by the hidden neurons per unit time during training.

and GEM-VLSNN improves test performance. For this classification task, where the model consists of a small number of read-out visible neurons, the difference in performance among the proposed training schemes is largely due to their different use of learning signals for the hidden neurons. Specifically, in terms of the estimated test log-likelihood, per-parameter learning signals in IW-VLSNN outperforms per-compartment learning signals in IW-VLSNN-b for small K , even while having the smallest communication load; while the use of per-compartment learning signals is seen to enhance the performance for large K . Finally, it is observed that the proposed schemes provide different trade-offs between costs (in terms of communication load and energy consumption) and learning performance (in terms of test log-likelihood and accuracy).

IX. CONCLUSIONS

In this paper, we have explored probabilistic spiking neural models in which each spiking neuron contains multiple compartments, each generating independent spiking outputs, while

sharing the same synaptic weights across compartments. We have introduced variational online learning rules that can leverage the presence of multiple compartments through importance weighting or generalized expectation-maximization. The learning rules are derived from the optimization of bounds on the likelihood and they rely on different form of feedback signals to visible and hidden neurons. Experiments on the neuromorphic data set MNIST-DVS have demonstrated that multi-compartment SNN, trained with the proposed learning rules can improve training and test performance.

While this work considered the log-likelihood of specific desired output spiking signals as the learning criterion, similar rules can be derived by considering other reward functions, such as Van Rossum (VR) distance [17], [44]. The multi-compartment SNN models and algorithms proposed in this paper can be also extended to networks of spiking Winner-Take-All (WTA) circuits [24], [26], which process multi-valued spikes.

REFERENCES

- [1] K. Hao, "Training a single ai model can emit as much carbon as five cars in their lifetimes," *MIT Technology Review*, 2019.
- [2] E. Strubell, A. Ganesh, and A. McCallum, "Energy and policy considerations for deep learning in nlp," *arXiv preprint arXiv:1906.02243*, 2019.
- [3] C. Mead, "Neuromorphic electronic systems," *Proceedings of the IEEE*, vol. 78, no. 10, pp. 1629–1636, 1990.
- [4] P. A. Merolla, J. V. Arthur, R. Alvarez-Icaza, A. S. Cassidy, J. Sawada, F. Akopyan, B. L. Jackson, N. Imam, C. Guo, Y. Nakamura *et al.*, "A million spiking-neuron integrated circuit with a scalable communication network and interface," *Science*, vol. 345, no. 6197, pp. 668–673, 2014.
- [5] M. Davies *et al.*, "Loihi: A neuromorphic manycore processor with on-chip learning," *IEEE Micro*, vol. 38, no. 1, pp. 82–99, 2018.
- [6] BrainChip, "Akida Neuromorphic System-on-Chip." [Online]. Available: <https://www.brainchipinc.com/products/akida-neuromorphic-system-on-chip>
- [7] E. O. Neftci, H. Mostafa, and F. Zenke, "Surrogate gradient learning in spiking neural networks: Bringing the power of gradient-based optimization to spiking neural networks," *IEEE Signal Processing Magazine*, vol. 36, no. 6, pp. 51–63, 2019.
- [8] P. Blouw, X. Choo, E. Hunsberger, and C. Eliasmith, "Benchmarking keyword spotting efficiency on neuromorphic hardware," in *Proceedings of Annual Neuro-inspired Computational Elements Workshop*, 2019, pp. 1–8.
- [9] N. Imam and T. A. Cleland, "Rapid online learning and robust recall in a neuromorphic olfactory circuit," *Nature Machine Intelligence*, vol. 2, no. 3, pp. 181–191, 2020.
- [10] D. Huh and T. J. Sejnowski, "Gradient descent for spiking neural networks," in *Proceedings of Advances in Neural Information Processing Systems*, 2018, pp. 1433–1443.
- [11] D. R. Jimenez, W. Gerstner *et al.*, "Stochastic variational learning in recurrent spiking networks," *Frontiers in Computational Neuroscience*, vol. 8, pp. 38–38, 2014.
- [12] J. Brea, W. Senn, and J.-P. Pfister, "Matching recall and storage in sequence learning with spiking neural networks," *Journal of Neuroscience*, vol. 33, no. 23, pp. 9565–9575, 2013.

- [13] H. Jang, O. Simeone, B. Gardner, and A. Grüning, “An introduction to probabilistic spiking neural networks: Probabilistic models, learning rules, and applications,” *IEEE Signal Processing Magazine*, vol. 36, no. 6, pp. 64–77, 2019.
- [14] J. Kaiser, H. Mostafa, and E. Neftci, “Synaptic plasticity dynamics for deep continuous local learning (decolle),” *arXiv preprint arXiv:1811.10766*, 2018.
- [15] S. M. Bohte, J. N. Kok, and H. La Poutre, “Error-backpropagation in temporally encoded networks of spiking neurons,” *Neurocomputing*, vol. 48, no. 1-4, pp. 17–37, 2002.
- [16] T. K. Moon, “The expectation-maximization algorithm,” *IEEE Signal Processing Magazine*, vol. 13, no. 6, pp. 47–60, 1996.
- [17] F. Zenke and S. Ganguli, “Superspike: Supervised learning in multilayer spiking neural networks,” *Neural Computation*, vol. 30, no. 6, pp. 1514–1541, 2018.
- [18] Y. Burda, R. Grosse, and R. Salakhutdinov, “Importance weighted autoencoders,” *arXiv preprint arXiv:1509.00519*, 2015.
- [19] Y. Tang and R. R. Salakhutdinov, “Learning stochastic feedforward neural networks,” in *Proceedings of Advances in Neural Information Processing Systems*, 2013, pp. 530–538.
- [20] A. Mnih and D. Rezende, “Variational inference for Monte Carlo objectives,” in *Proceedings of International Conference on Machine Learning*, 2016, pp. 2188–2196.
- [21] J. Domke and D. R. Sheldon, “Importance weighting and variational inference,” in *Proceedings of Advances in Neural Information Processing Systems*, 2018, pp. 4470–4479.
- [22] J. A. Nelder and R. W. Wedderburn, “Generalized linear models,” *Journal of the Royal Statistical Society: Series A (General)*, vol. 135, no. 3, pp. 370–384, 1972.
- [23] N. Frémaux and W. Gerstner, “Neuromodulated spike-timing-dependent plasticity, and theory of three-factor learning rules,” *Frontiers in Neural Circuits*, vol. 9, p. 85, 2016.
- [24] H. Mostafa and G. Cauwenberghs, “A learning framework for winner-take-all networks with stochastic synapses,” *Neural Computation*, vol. 30, no. 6, pp. 1542–1572, 2018.
- [25] S. Guo, Z. Yu, F. Deng, X. Hu, and F. Chen, “Hierarchical Bayesian inference and learning in spiking neural networks,” *IEEE Transactions on Cybernetics*, vol. 49, no. 1, pp. 133–145, 2017.
- [26] H. Jang, N. Skatchkovsky, and O. Simeone, “VOWEL: A local online learning rule for recurrent networks of probabilistic spiking winner-take-all circuits,” *arXiv preprint arXiv:2004.09416*, 2020.
- [27] G. B. Ermentrout and D. H. Terman, *Mathematical foundations of neuroscience*. Springer Science & Business Media, 2010, vol. 35.
- [28] D. Driessens, V. V. Hafner, and M. Schmuker, “Sparse coding with a somato-dendritic rule,” *BioRxiv*, p. 451955, 2018.
- [29] S. B. Furber, D. R. Lester, L. A. Plana, J. D. Garside, E. Painkras, S. Temple, and A. D. Brown, “Overview of the spinnaker system architecture,” *IEEE Transactions on Computers*, vol. 62, no. 12, pp. 2454–2467, 2012.
- [30] J. W. Pillow, J. Shlens, L. Paninski, A. Sher, A. M. Litke, E. Chichilnisky, and E. P. Simoncelli, “Spatio-temporal correlations and visual signalling in a complete neuronal population,” *Nature*, vol. 454, no. 7207, pp. 995–999, 2008.
- [31] K. Doya, S. Ishii, A. Pouget, and R. P. Rao, *Bayesian brain: Probabilistic approaches to neural coding*. MIT press, 2007.
- [32] T. Osogami and M. Otsuka, “Learning dynamic boltzmann machines with spike-timing dependent plasticity,” *arXiv preprint arXiv:1509.08634*, 2015.
- [33] D. Koller and N. Friedman, *Probabilistic graphical models: principles and techniques*. MIT press, 2009.
- [34] J. Peters and S. Schaal, “Reinforcement learning of motor skills with policy gradients,” *Neural Networks*, vol. 21, no. 4, pp. 682–697, 2008.
- [35] G. Kramer, *Directed information for channels with feedback*. Hartung-Gorre, 1998.
- [36] C. M. Bishop, *Pattern recognition and machine learning*. Springer, 2006.

- [37] O. Simeone, “A brief introduction to machine learning for engineers,” *Foundations and Trends® in Signal Processing*, vol. 12, no. 3-4, pp. 200–431, 2018.
- [38] T. Serrano-Gotarredona and B. Linares-Barranco, “Poker-dvs and mnist-dvs. their history, how they were made, and other details,” *Frontiers in Neuroscience*, vol. 9, p. 481, 2015.
- [39] C. Guo, G. Pleiss, Y. Sun, and K. Q. Weinberger, “On calibration of modern neural networks,” *arXiv preprint arXiv:1706.04599*, 2017.
- [40] P. Lichtsteiner, C. Posch, and T. Delbruck, “A 128 x 128 120db 30mw asynchronous vision sensor that responds to relative intensity change,” in *2006 IEEE International Solid State Circuits Conference-Digest of Technical Papers*. IEEE, 2006, pp. 2060–2069.
- [41] B. Zhao, R. Ding, S. Chen, B. Linares-Barranco, and H. Tang, “Feedforward categorization on aer motion events using cortex-like features in a spiking neural network,” *IEEE Transactions on Neural Networks and Learning Systems*, vol. 26, no. 9, pp. 1963–1978, 2014.
- [42] J. A. Henderson, T. A. Gibson, and J. Wiles, “Spike event based learning in neural networks,” *arXiv preprint arXiv:1502.05777*, 2015.
- [43] C. M. Bishop, “Mixture density networks,” 1994.
- [44] M. v. Rossum, “A novel spike distance,” *Neural Computation*, vol. 13, no. 4, pp. 751–763, 2001.